Available online at www.sciencedirect.com
ScienceDirect
Biosensors and Bioelectronics 22 (2007) 933–940
BIOSENSORS & BIOELECTRONICS
www.elsevier.com/locate/bios

Direct labeling microRNA with an electrocatalytic moiety and its application in ultrasensitive microRNA assays

Zhiqiang Gao [a,*], Yuan Hong Yu [b]

[a] *Institute of Microelectronics, A*STAR, 11 Science Park Road, Singapore 117685, Singapore*
[b] *Centre for Molecular Medicine, A*STAR, 61 Biopolis Drive, Singapore 138673, Singapore*

Received 3 January 2006; received in revised form 30 March 2006; accepted 5 April 2006
Available online 2 June 2006

Abstract

An ultrasensitive procedure for the detection of microRNA (miRNA) in total RNA is described in this work. The miRNA is directly labeled with a redox active and electrocatalytic moiety, $Ru(PD)_2Cl_2$ (PD = 1,10-phenanthroline-5,6-dione), through coordinative bonds with purine bases in the miRNA molecule. The excellent electrocatalytic activity of the $Ru(PD)_2Cl_2$ towards the oxidation of hydrazine makes it possible to conduct ultrasensitive miRNA detection. Under optimized experimental conditions, the assay allows the detection of miRNAs in the range of 0.50–400 pM with a detection limit of 0.20 pM in 2.5 μl (0.50 amole). MicroRNA quantitation is therefore performed in as little as 10 ng of total RNA, providing a much-needed platform for miRNA expression analysis.

Keywords: MicroRNA; Electrocatalysis; Amperometry; 1,10-Phenanthroline-5,6-dione; Ruthenium

1. Introduction

MicroRNAs comprise a group of noncoding 18–25 nucleotide RNAs (Bartel, 2004). Recent progress in miRNA research has shown that miRNAs regulate a wide range of biological functions from cell proliferation and death to cancer progression (Bartel, 2004; Lu et al., 2005). It is widely believed that miRNA expression analysis is the key to its physiological functions. There is an urgent need for a reliable and ultrasensitive method for miRNA expression analysis. Northern blot is the most commonly used method in expression analysis of both mature and precursor miRNAs, since it allows gene expression quantification and miRNA size determination (Lagos-Quintana et al., 2001; Lee and Ambros, 2001; Reinhart et al., 2000; Calin et al., 2002). However, the low sensitivity and laborious procedures of Northern blot make it difficult for routine miRNA analysis. RT-PCR can theoretically amplify a single nucleic acid molecule millions of times and thus is very useful for very small sample size and low abundance genes. Unfortunately, the short length and low abundance of miRNA render PCR-based tools ineffective because much shorter primers do not effectively bind to such short miRNA templates (Liu et al., 2004; Calin et al., 2004). RT-PCR is restricted to the detection of miRNA precursors (Schmittgen et al., 2004). Although miRNA precursors do shed some light on miRNA transcript regulation, it does not represent the exact expression profile of active mature miRNAs, because miRNA precursors have to undergo several processes before they are in biologically active forms. Therefore, direct quantitation of the mature miRNAs is more representative, desirable, and reliable.

In view of the extremely small size of miRNAs, direct labeling miRNAs themselves may be more advantageous. Recently, Babak and co-workers proposed a cisplatin-based chemical labeling procedure for miRNAs (Babak et al., 2004). One binding site of cisplatin is covalently bound to a fluorophore and the other site is a labile nitrate ligand. Incubation in an aqueous solution with miRNAs at elevated temperatures results in a ligand exchange between the labile nitrate of the cisplatin complex and the more strongly coordinating purine moiety, forming a new complex between cisplatin and the N_7 position of G base. The miRNA was therefore directly labeled with the cisplatin–fluorophore conjugate through a coordinative bond with G base in miRNA. Another direct labeling procedure at the 3′ end was recently developed by Liang et al. in which miRNAs

* Corresponding author. Tel.: +65 6770 5928; fax: +65 6773 1914.
E-mail address: gaozq@ime.a-star.edu.sg (Z. Gao).

0956-5663/$ – see front matter © 2006 Published by Elsevier B.V.
doi:10.1016/j.bios.2006.04.020

were first tagged with biotin. After the introduction of quantum dots to the hybridized miRNAs through a reaction with quantum dots–avidin conjugates, the miRNAs were detected fluorescently with a dynamic range from 156 pM to 20 nM (Liang et al., 2005). Thomson's group used T4 RNA ligase to couple the 3′ end of miRNA to a fluorophore-tagged nucleotide (Thomson et al., 2004). Overall, the direct ligation procedures do not offer the much-needed sensitivity for miRNA expression analysis.

To further enhance the sensitivity and lower the detection limit, we believe that a chemical or biological amplification scheme must be employed in the direct ligation procedures. It has been demonstrated that the sensitivity of the amplified electrochemical detection of nucleic acids is comparable to that of PCR-based fluorescent assays (Zhang et al., 2003; Xie et al., 2004a,b). However, of the many proposed amplified electrochemical schemes, only a few reports dealed with the detection of RNA, and mRNA in particular (Xie et al., 2004a,b; Piunno and Krull, 2005). So far, no attempts have been made in electrochemical miRNA assay. In this report, we present a novel labeling procedure that utilizes a chemical ligation to directly label miRNA with a redox active and catalytic moiety. The miRNA is labeled in total RNA mixture in a one-step non-enzymatic reaction under very mild conditions. The amplification from the electrocatalytic oxidation of hydrazine greatly enhances the detectability of the assay, thereby lowering the detection limit to 0.20 pM.

2. Materials and methods

2.1. Materials

Unless otherwise stated, reagents were obtained from Sigma–Aldrich (St. Louis, MO) and used without further purification. $Ru(PD)_2Cl_2$ was synthesized from $RuCl_3$ according to a literature procedure (Goss and Abruna, 1985). A phosphate buffered-saline (PBS, pH 8.0), consisting of 0.15 M NaCl and 20 mM phosphate buffer, was used for washing and electrochemical measurements. To minimize the effect of RNases on the stability of miRNAs, all solutions were treated with diethyl pyrocarbonate and surfaces were decontaminated with RNaseZap (Ambion, TX). Since the labeling process is only effective to G and A bases, three representative human miRNAs let-7b, mir-92 and mir-320, covering the entire range of 30–80% (G + A) content of known human miRNAs (Griffiths-Jones, 2004), were selected as our target miRNAs. Aldehyde-modified oligonucleotide capture probes used in this work were custom-made by Invitrogen Corporation (Carlsbad, CA) and all other oligonucleotides of PCR purity were custom-made by Proligo (Boulder, CO). Indium tin oxide (ITO) coated glass slides were from Delta Technologies Limited (Stillwater, MN).

2.2. Apparatus

Electrochemical experiments were carried out using a CH Instruments model 660A electrochemical workstation (CH Instruments, Austin, TX). A conventional three-electrode system, consisting of an ITO working electrode, a non-leak Ag/AgCl (3.0 M NaCl) reference electrode (Cypress Systems, Lawrence, KS), and a platinum wire counter electrode, was used in all electrochemical measurements. All potentials reported in this work were referred to the Ag/AgCl electrode. Electrospray ionization mass spectrometric (ESI-MS) experiments were performed with a Finnigan/MAT LCQ Mass Spectrometer (ThermoFinnigan, San Jose, CA). Inductively coupled plasma-mass spectrometry (ICP-MS) was conducted with an Elan DRC II ICP-MS spectrometer (PerkinElmer, Wellesley, MA). UV–vis spectra were recorded on a V-570 UV/VIS/NIR spectrophotometer (JASCO Corp., Japan). All experiments were carried out at room temperature, unless otherwise stated.

2.3. Total RNA extraction and labeling

Total RNA from human HeLa cells were extracted using TRIzol reagent (Invitrogen, Carlsbad, CA) according to the manufacturer's recommended protocol. MicroRNAs in the total RNA were enriched using a Montage spin column YM-50 column (Millipore Corporation). RNA concentration was determined by UV–vis spectrophotometry. Typically, 1.0 μg of total RNA was used in each of the labeling reactions. To 5.0 μl of total RNA solution was added 20 μl of 0.25 mM $Ru(PD)_2Cl_2$ in 0.10 M pH 6.0 acetate buffer. The mixture was incubated for 30–40 min at 80 °C and cooled on ice. The labeled RNA was stored at −20 °C after adding 5.0 μl of 3.0 M KCl.

2.4. Electrode preparation, hybridization and detection

The pretreatment, silanization and oligonucleotide capture probes immobilization of the ITO electrode were as previously described (Gao and Tansil, 2005). The surface density of the immobilized capture probes was $(6.0–8.5) \times 10^{-12}$ mol/cm^2. As schematically illustrated in Fig. 1, the miRNA assay was carried out as follows: first, the electrode was placed in a moisture saturated environmental chamber maintained at 30 °C. A 2.5 μl aliquot of hybridization solution, containing the desired amount of labeled miRNA, was uniformly spread onto the electrode. It was then rinsed thoroughly with a blank hybridization solution at 30 °C after a 60-min of hybridization period. The hydrazine electrooxidation current was measured amperometrically at 0.10 V in vigorously stirred PBS containing 5.0 mM hydrazine. At low miRNA concentrations, smoothing was applied after each amperometric measurement to remove random noise and electromagnetic interference.

3. Results and discussion

3.1. Feasibility of direct labeling miRNA with $Ru(PD)_2Cl_2$

The $Ru(PD)_2Cl_2$ complex is stable under ambient conditions, but may undergo ligand exchange with other ligands at elevated temperatures, as with many other similar ruthenium complexes (Seddon and Seddon, 1984). It is well known that ruthenium complexes tend to selectively bind to imine sites in biomolecules (Clarke, 2002). For example, they often selectively form coordinative bonds with histidyl imidazole nitrogens on proteins and the N_7 site on the imidazole ring of

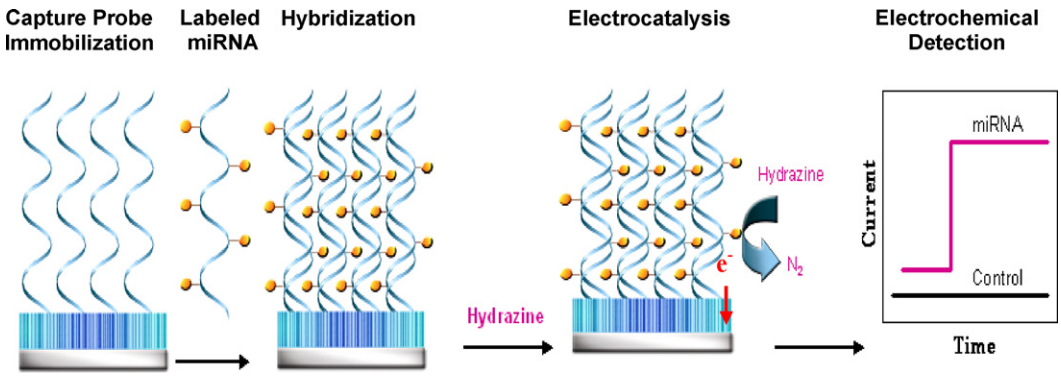

Fig. 1. Schematic representation of a miRNA assay using electrocatalytic label.

purine nucleotides (Gray and Winkler, 1996). The substitution of chloride in $Ru(PD)_2Cl_2$ by nucleic acids is believed to be similar to that of cisplatin (Xie et al., 2004b). A direct proof of the formation of nucleotide–$Ru(PD)_2Cl_2$ adduct would be mass spectrometry. Thus, we first conducted a series of mass spectrometric tests on $Ru(PD)_2Cl_2$ treated nucleotides, the simplest RNA model compounds. ESI-MS was used to characterize the chemistry between $Ru(PD)_2Cl_2$ and nucleotides because of its mild ionization process. As depicted in Fig. 2, among the four nucleotides tested, only guanosine 5′-monophosphate (GMP) and adenosine 5′-monophosphate (AMP) produced new ion clusters at *m*/*z* 868 and 884, which were assigned to $[GMP–Ru(PD)_2]^+$ and $[AMP–Ru(PD)_2]^+$, respectively, based on the excellent match between the experimental and calculated isotopic distribution patterns and the molecular weights of the adducts (Fig. 2). ESI-MS tests suggest that only AMP and GMP readily undergo ligand exchange with the chloride in $Ru(PD)_2Cl_2$. Moreover, the molecular clusters of double-exchanged $Ru(PD)_2Cl_2$–nucleotide adducts were not observed even after a prolonged incubation at 80 °C, indicating that $Ru(PD)_2Cl_2$ undergoes only mono-substitution under the experimental conditions even though it has two *cis* coordinating labile chloride ligands. The inability of double-ligand exchange is most probably due to steric constraints of $Ru(PD)_2Cl^+$ that hinders the binding of more than one purine base, as previously observed in similar ruthenium complexes (Hotze et al., 2000). Double-ligand exchange with the sterically more hindered six-coordinated octahedral ruthenium complexes is evidently much more difficult than it is for square-planar platinum complexes, such as cisplatin (Xie et al., 2004b). However, mono-substitution is actually a desirable feature in developing chemical ligation procedures for miRNA assays because it offers an excellent control over the ligation process and prevents "cross-linking" between miRNA molecules (intermolecular cross-linking) and between purine bases of the same miRNA molecule (intramolecular cross-linking). As expected, intermolecular cross-linking will greatly affect hybridization efficiency and intramolecular cross-linking alter the miRNA sequence by generating "loops" in the miRNA strand.

As discussed above, mass spectrometric data clearly indicate that $Ru(PD)_2Cl_2$ can be grafted onto nucleotides via ligand exchange under mild conditions. However, the introduction of $Ru(PD)_2Cl_2$ onto oligonucleotides might severely affect hybridization efficiency. To ensure that the labeled oligonucleotides retain their biological integrity, a series of gel electrophoretic tests were performed on oligonucleotides after

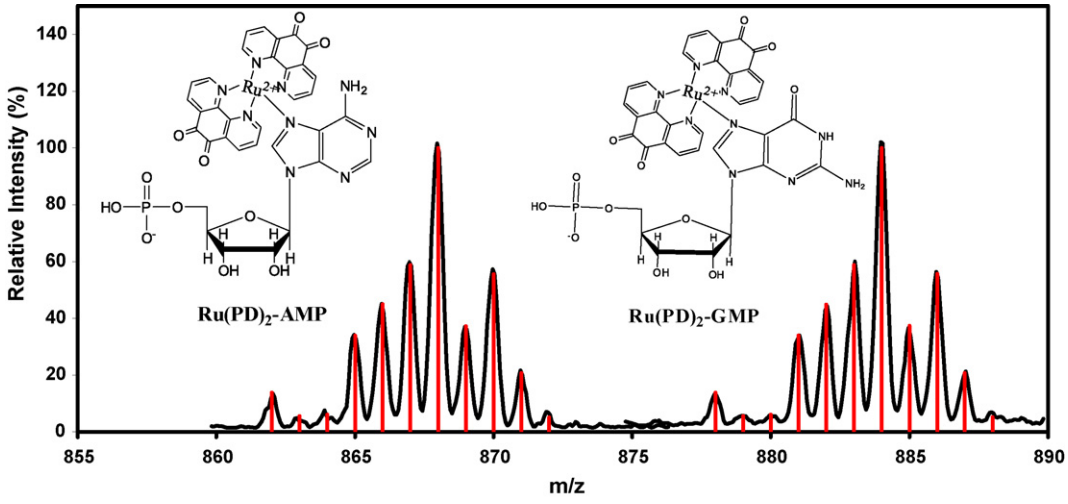

Fig. 2. Mass spectra of $Ru(PD)_2Cl_2$ treated nucleotides (black) and calculated isotopic distribution patterns (red). (For interpretation of the references to colour in this figure legend, the reader is referred to the web version of the article.)

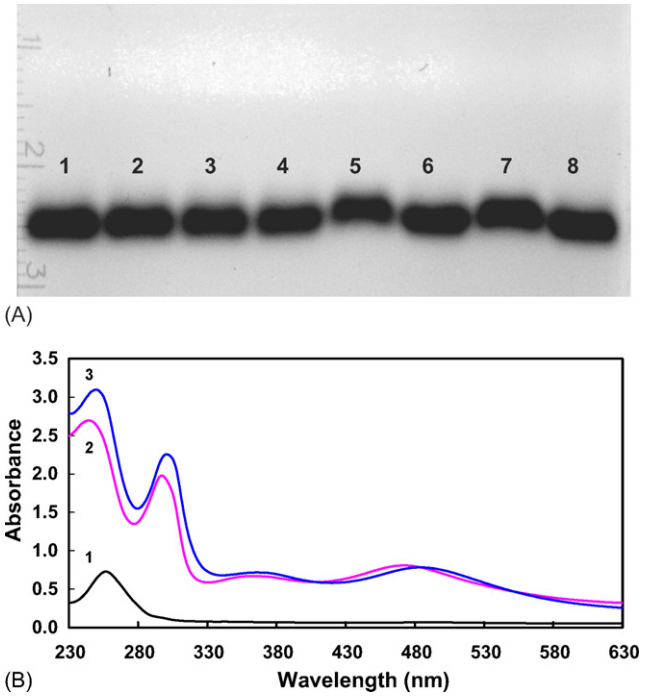

Fig. 3. (A) Gel electrophoresis of oligonucleotides. (1) poly(A)$_{30}$ + poly(U)$_{30}$ and (2) poly(G)$_{30}$ + poly(C)$_{30}$; (3) poly(A)$_{30}$ + poly(U)$_{30}$ and (4) poly(G)$_{30}$ + poly(C)$_{30}$ incubated with Ru(PD)$_2$Cl$_2$ at room temperature for 120 min; (5) poly(A)$_{30}$, (6) poly(U)$_{30}$, (7) poly(G)$_{30}$ and (8) poly(C)$_{30}$ incubated with Ru(PD)$_2$Cl$_2$ at 80 °C for 30 min and hybridized with their untreated complementary oligonucleotides, respectively. (B) UV–vis spectra of (1) 3.3 μM poly(A)$_{30}$, (2) 100 μM Ru(PD)$_2$Cl$_2$, and (3) 100 μM Ru(PD)$_2$Cl$_2$ treated 3.3 μM Poly(A)$_{30}$.

Ru(PD)$_2$Cl$_2$ treatments. As illustrated in lanes 1–4 in Fig. 3A, little difference was observed between untreated oligonucleotides and those after prolonged incubations with Ru(PD)$_2$Cl$_2$ at room temperature, implying that no ligand exchange occurs at room temperature and Ru(PD)$_2$Cl$_2$ has little effect on the biological function of the oligonucleotides. On the other hand, distinct changes were obtained among the four oligonucleotides after a 30-min incubation with Ru(PD)$_2$Cl$_2$ at 80 °C. The electrophoretic mobility of the treated poly(A)$_{30}$ and poly(G)$_{30}$ is slower than that of poly(U)$_{30}$ and poly(C)$_{30}$ (lanes 5–8), suggesting that additional mass and/or positive charges are added onto these oligonucleotides. Gel electrophoresis confirms that Ru(PD)$_2$Cl$_2$ is successfully grafted onto poly(A)$_{30}$ and poly(G)$_{30}$. More importantly, the presence of Ru(PD)$_2$Cl$^+$ labels in the oligonucleotides posts little hindrance on hybridization efficiency, paving the way for the development of ultrasensitive miRNA assay. Under identical experimental conditions, little difference was observed between Ru(PD)$_2$Cl$_2$ labeled poly(A)$_{30}$ and poly(G)$_{30}$, indicating that purine bases in poly(A)$_{30}$ and poly(G)$_{30}$ are equally reactive at 80 °C. At lower temperatures and/or shorter reaction times poly(G)$_{30}$ is slightly more reactive than poly(A)$_{30}$ reflected by a slightly slower migration. In contrast, the poly(U)$_{30}$ and ploy(C)$_{30}$ showed little difference from their untreated counterparts (lanes 1, 2, 6 and 8), implying that Ru(PD)$_2$Cl$_2$ is inactive to these oligonucleotides. Quantitative analysis using ICP-MS revealed that 28–32% of the G and A bases in the oligonucleotides are successfully labeled. Later experiments showed that this labeling efficiency is sufficient for ultrasensitive miRNA assays. From the above data, it is clear that the labeling efficiency is miRNA sequence-dependent since Ru(PD)$_2$Cl$_2$ can only label miRNAs with G and A bases in them with an efficiency of ~30%. In extreme cases where there are no A and G bases in the miRNAs this labeling procedure will fail. Fortunately, there are no known miRNAs that lack G and A bases (Griffiths-Jones, 2004).

Fig. 3B illustrates the UV–vis absorption spectra of the starting materials and the labeled oligonucleotide, taking poly(A)$_{30}$ as an example. The spectrum of the oligonucleotide before labeling showed the typical transition of the heterocyclic oligonucleotides around 260 nm (Fig. 3B, trace 1). The spectrum of Ru(PD)$_2$Cl$_2$ is more or less characteristic of the spectra for Ru–PD complexes. It exhibits two intense bands in the UV region due to ligand localized π–π^* transitions. The same transitions are found in free PD (Goss and Abruna, 1985). The two board bands in the regions 330–400 and 430–600 nm are due to spin allowed Ru(dπ) → PD(π^*) metal-to-ligand charge-transfer (MLCT) transitions (Fig. 3B, trace 2). The spectrum of the labeled oligonucleotide appeared as a superposition of the oligonucleotide and Ru(PD)$_2$Cl$_2$ with some red shift of ~15 nm in the 430–600 nm region (Fig. 3B, trace 3). This is likely a direct consequence of the ligand exchange. The purine group is conjugated, resulting in a lower π^* level for this ligand relative to the chloride of the complex, again confirming the formation of the Ru(PD)$_2$Cl$_2$–poly(A) adduct.

3.2. Hybridization and feasibility study of miRNA detection

Nucleic acid assays with electrocatalytic labels have previously been reported (Tansil et al., 2005). The labels chemically amplify analytical signals to hybridized electrodes compared to non-hybridized ones. The difference in amperometric currents is used for quantitation purpose. In a similar way, Ru(PD)$_2$Cl$^+$ was evaluated as a novel electrocatalytic label for possible applications in ultrasensitive miRNA assays.

Thermal melting was first conducted between 20 and 70 °C to evaluate the stability of the hybridized oligonucleotides before looking into the feasibility of electrocatalytic assays for miRNAs. A mixture of the complementary oligonucleotide strands was first heated to 70 °C and then slowly cooled down to room temperature. It was found that the presence of Ru(PD)$_2$Cl$^+$ in the oligonucleotides slightly destabilizes the duplex when compared to their unlabeled counterparts, $\Delta T_m = -1.0$ °C for poly(G)$_{30}$ and −2 °C for poly(A)$_{30}$. Several factors may possibly contribute to the slightly reduced stability of the labeled oligonucleotides. These include electrostatic interaction, steric hindrance and solvation. The introduction of cationic Ru(PD)$_2$Cl$^+$ is expected to stabilize the duplex by reducing net electrostatic repulsion between the two strands, while the presence of the bulky labels and the aromatic ligands in the major groove may reduce the stability of the duplex by repelling water molecules and bound small cations. From the thermal melting experiments, it is evident that most of the destabilization effect is compensated by the electrostatic interaction.

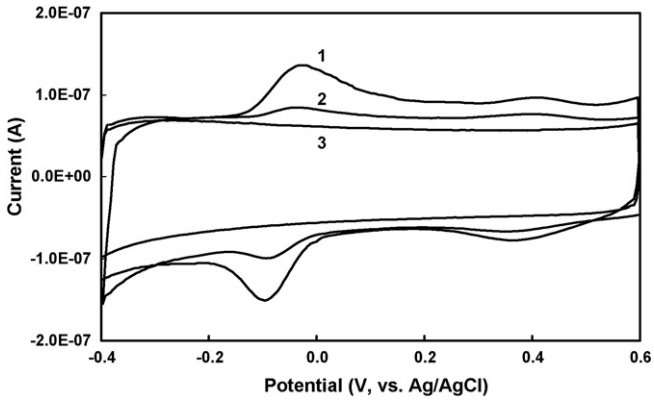

Fig. 4. Voltammograms of $Ru(PD)_2Cl_2$ treated with: (1) 50 nM let-7b, (2) 10 nM let-7b, and (3) 50 nM mir-92 at electrodes complementary to let-7b. Supporting electrolyte PBS buffer, potential scan rate 100 mV/s.

In the first hybridization tests, electrodes coated with capture probes complementary to let-7b were used to analyze let-7b and mir-92 (non-complementary, control). Upon hybridization, the complementary let-7b labeled with $Ru(PD)_2Cl_2$ was selectively bound to the capture probes and became fixed on the electrode surface. On the contrary, little if any of the non-complementary mir-92 was captured during hybridization, hence minute voltammetric response of the electrode was expected. It was found that extensive washing with a NaCl-saturated phosphate buffer (pH 6.0) containing 0.10 mM ascorbic acid removed most of the non-miRNA related $Ru(PD)_2Cl_2$ uptake from the labeling solution since there is little interaction between the neutral $Ru(PD)_2Cl_2$ and oligonucleotides on the electrode surface. Cyclic voltammograms for the electrodes after hybridization to let-7b and mir-92 are shown in Fig. 4. No obvious voltammetric activities were obtained after hybridization to mir-92 (Fig. 4, trace 3), indicating that there is very little non-hybridization-related uptake of mir-92 and/or $Ru(PD)_2Cl_2$. As shown in traces 1 and 2 in Fig. 4, after hybridization to different amounts of let-7b miRNA, two pairs of voltammetric peaks were observed and the peak currents were directly proportional to the concentration of let-7b. The current peaks near −0.10 V are due to the redox processes of the coordinated PD ligands and those at 0.40 V to the redox processes of the metal center (Goss and Abruna, 1985). These results clearly demonstrates that the labeled miRNA selectively hybridizes with its complementary capture probe on the electrode surface with very little cross-hybridization. Consequently, the usage of $Ru(PD)_2Cl^+$ as a redox active indicator for the direct detection of miRNA was evaluated. A detection limit of 2.0 nM and a dynamic range up to 500 nM were obtained. The hybridization efficiency at the high end of the dynamic range was evaluated electrochemically using the $Ru(PD)_2Cl^+$ label on the miRNA. The number of $Ru(PD)_2Cl^+$ molecules producing the observed current was estimated from the charge under the first oxidation current peak. Since four electrons are transferred per label, the observed current of 0.49 μA after hybridization to 500 nM of the complementary target miRNA, resulted therefore from 1.9 pmol of active $Ru(PD)_2Cl^+$ labels. Assuming a $Ru(PD)_2Cl^+$/RNA base pair ratio of ∼1/3, the hybridization efficiency was found to be ∼23%, corresponding to ∼26% of target miRNA in the sample droplet, which is comparable to the values found in the literature (Xie et al., 2004a,b; Tansil et al., 2005; Caruso et al., 1997).

In the second set of experiments, the electrodes were evaluated voltammetrically in PBS containing 0.10 mM hydrazine before and after hybridization. Fig. 5A shows cyclic voltammograms of hydrazine at the electrode before (Fig. 5A, trace 1) and after hybridization (Fig. 5A, trace 3). For comparison, a voltammogram of the hybridized electrode in blank PBS is also presented (Fig. 5A, trace 2). Both electrodes showed a totally irreversible oxidation process for hydrazine. Before

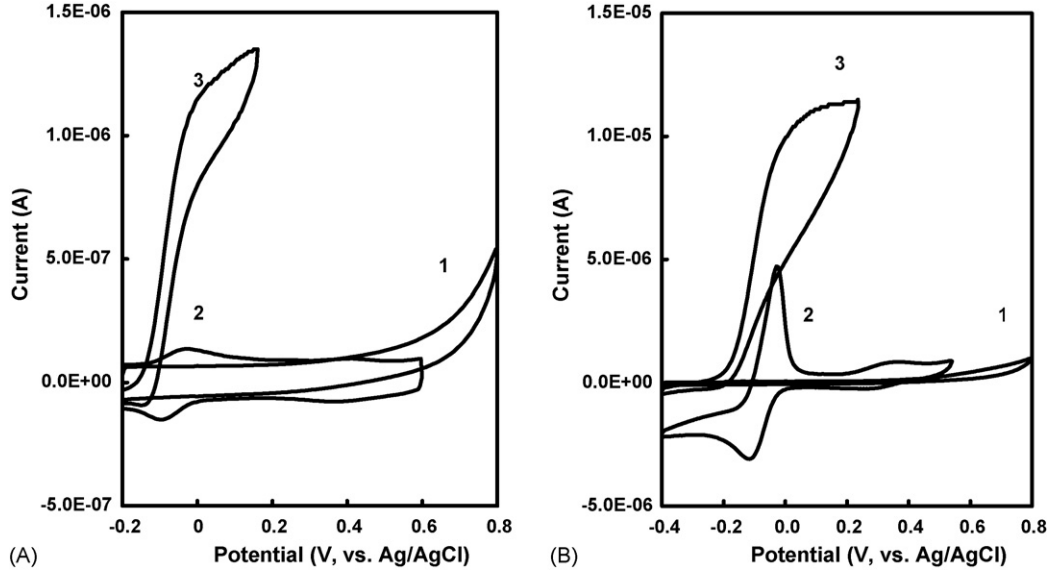

Fig. 5. (A) Cyclic voltammograms of 0.10 mM hydrazine at a capture probe coated electrode (1) before and (3) after hybridization to its complementary 50 nM let-7b, and (2) the hybridized electrode in blank PBS. (B) Cyclic voltammograms of 1.0 mM hydrazine at a blank ITO electrode (1) in the absence and (3) in the presence of 0.10 mM $Ru(PD)_2Cl_2$, and (2) $Ru(PD)_2Cl_2$ at the blank ITO electrode. Supporting electrolyte PBS, potential scan rate 100 mV/s.

hybridization the anodic peak potential (E_p) for hydrazine oxidation is beyond 0.80 V, largely due to oxidation overpotential and the presence of MD and anionic oligonucleotide capture probes. Both of them substantially impede electron exchange between the underlying electrode and hydrazine. It can be seen that the presence of $Ru(PD)_2Cl^+$ greatly reduces the overpotential of hydrazine oxidation, shifting the E_p value negatively by as much as 850 mV to −0.050 V, most likely due to the catalytic effect of PD ligands in the labels. To ensure that the enhanced current is indeed form the genuine electrocatalysis of hydrazine, voltammetric tests were conducted in homogeneous $Ru(PD)_2Cl_2$ solution. A cyclic voltammogram recorded with a blank ITO electrode in a 0.10 mM solution of $Ru(PD)_2Cl_2$ is shown in trace 2 in Fig. 5B. It is seen that the first oxidation peak is much higher and sharper than other peaks due to strong adsorption of $Ru(PD)_2Cl_2$, a phenomenon previously studied by Anson (Shi and Anson, 1998). Because four electrons are involved in the reduction of the two PD ligands coordinated to each ruthenium center, the cathodic peak at −0.10 V, produced by the reduction of PD ligands in the complex is much larger than peaks for the Ru(III)/Ru(II) processes at ∼0.30 V. The single cathodic peak, instead of two separate peaks, suggests equality of the two PD ligands. In other words, the two PD ligands in the complex interact with the metal center approximately equally and they do not interact strong enough with each other to alter their redox potential substantially; hence the two PD ligands are reduced in a single, four-electron step consisting of two simultaneous two-electron reductions of the two PD ligands. Theoretically, the cathodic peak current would be expected to be $2^{3/2} \times 2 = 5.6$ times as large as the peak current for the one-electron oxidation of Ru(II) to Ru(III) (Bard and Faulkner, 2001). The actual ratio of the peak current was not far from the theoretical value, but an exact match was not observed because of the complications from adsorption/desorption processes (Shi and Anson, 1998). It is well documented that the direct oxidation of hydrazine suffers from very large overpotentials. Reported values for its oxidation potential range from 0.40 to 1.0 V. In our case, the oxidation potential at the ITO electrode is >0.80 V (Fig. 5B, trace 1). In the presence of $Ru(PD)_2Cl_2$, however, a voltammogram of hydrazine, as shown in trace 3 in Fig. 5B, was obtained. The sinusoidal shape and the position of the voltammogram immediately suggest that there is a very strong catalytic effect by the metal complex since the current at potentials in the vicinity of the PD redox potential increases substantially, indicating that the complex is being turned over by the oxidation of hydrazine (Bard and Faulkner, 2001). The increase in peak current and the decrease in the anodic overpotential demonstrate an efficient electrocatalysis of hydrazine. The shift in the overpotential is due to a kinetic effect that greatly increases the rate of electron transfer from hydrazine to the electrode, which in turn is attributed to the improvement in the reversibility of the electron transfer processes. It was found that the current increases when increasing hydrazine concentration suggesting that the electrocatalytic effect is very efficient so that the overall process is solely controlled by the diffusion of hydrazine to the electrode.

On the basis of the above voltammetric investigations, it seems highly likely that better analytical characteristics can be achieved in amperometry. The feature of the electrocatalysis that appears to be particularly promising is the extremely low potential at which hydrazine oxidation takes place. Amperometric detection at significantly lower operating potentials minimizes potential interferences and reduces the background signal, yielding an improved signal/noise ratio and a lower detection limit. As demonstrated in Fig. 6, upon addition of

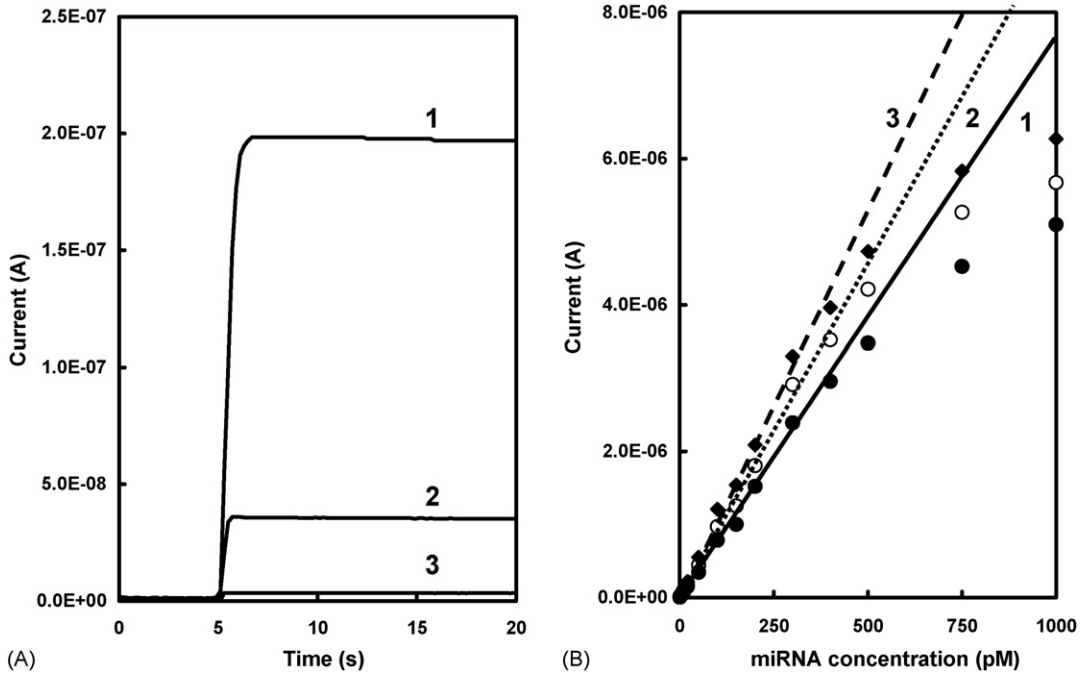

Fig. 6. (A) Amperometric curves of (1) 25 pM let-7b, (2) 25 pM let-7c, and (3) 25 pM mir-92 hybridized to capture probe coated electrodes complementary to let-7b. (B) Calibration curves for (1) mir-92, (2) let-7b, and (3) mir-320.

Table 1
Analysis of miRNAs in total RNA extracted from HeLa cells

	Let-7b (copy/μg RNA)	Mir-92 (copy/μg RNA)	Mir-320 (copy/μg RNA)
This method	$5.7 \pm 0.68 \times 10^7$	$3.6 \pm 0.51 \times 10^7$	$0.83 \pm 0.13 \times 10^7$
Northern blot	$5.5 \pm 0.60 \times 10^7$	$3.8 \pm 0.62 \times 10^7$	$0.75 \pm 0.15 \times 10^7$

5.0 mM hydrazine to PBS, the oxidation current in amperometry increased to 195 nA at 0.10 V at the electrode hybridized to 25 pM of the complementary target miRNA (Fig. 6A, trace 1), whereas the electrode hybridized with non-labeled miRNA gave an oxidation current practically indistinguishable from the background noise. Furthermore, in a control experiment that used the non-complementary target miRNA, only a 3.2 nA increment in hydrazine oxidation current was observed (Fig. 6A, trace 3), largely due to the residual non-hybridization-related uptake of $Ru(PD)_2Cl_2$. The specificity of the assay for detection of target miRNA was further evaluated by analyzing let-7b and let-7c with electrodes coated with capture probes complementary to let-7b. There is only one nucleotide difference (G ↔ A) out of 22 nucleotides of let-7b and let-7c (Griffiths-Jones, 2004). In other words, the capture probe for let-7b is one base-mismatched for let-7c. As shown in trace 2 in Fig. 6A, the current increment dropped by ~80% to as low as 36 nA when let-7c was tested on the electrode, readily allowing discrimination between the perfectly matched and mismatched miRNAs. The amperometric data agrees well with the voltammetric results obtained earlier and confirms that the target miRNA was successfully detected with high specificity and sensitivity. Therefore, each quantified result represents the specific quantity of a single miRNA member and not the combined quantity of the entire family.

3.3. Calibration curves for miRNAs

In this study, three representative miRNAs with a (G + A) content from 30 to 80%, covering the entire range of (G + A) content of known human miRNAs, were selected. Solutions of different concentrations of labeled miRNAs, ranging from 0.10 to 1000 pM, were tested. For the control experiments, non-complementary capture probes were used in the electrode preparation. As illustrated in Fig. 6B, the dynamic range was 0.50–400 pM, with relative standard deviations of 16–22% and a detection limit of 0.20 pM (0.50 amole). Compared to previous chemical ligation-based miRNA assays, the sensitivity of miRNA analysis was greatly improved by adopting the multiple labeling and chemical amplification schemes. In the assays reported earlier the ratio of label and target miRNA molecule was fixed at unit. The amount of capture probes immobilized on the electrode surface and hybridization efficiency determine the amount of target miRNA bound to the surface and thereby the amount of labels. However, in our proposed model, multiple $Ru(PD)_2Cl^+$ labels on a single miRNA strand greatly increases the label loading, proportionally increasing the response from electrocatalytic oxidation, and hence the sensitivity and detection limit of the miRNA assay were substantially improved. The label/base ratio was estimated to be in the range of 1/3 to 1/4 depending on the sequence of individual miRNA molecule. Theoretically, if this ratio keeps unchanged for all miRNAs, the same current sensitivity per base should be obtained for all miRNAs. At the same molar concentration, the sensitivity should be roughly proportional to the number of base in the miRNA, but this trend was not observed in our experiments. It is noteworthy that the sensitivity per base is dependent on miRNA sequence and (G + A) content. However, no straightforward relation between (G + A) content and current sensitivity was observed. This is probably due to the fact that G and A are not evenly distributed. Owing to the steric hindrance and three-dimensional packing of the miRNA molecules on the electrode surface, it would be impossible to label some of the G and A bases when they are in a cluster, so a low labeling efficiency is expected. For example, the (G + A) content (78%) in mir-320 is more than doubled as compared to that of mir-92, but the sensitivity for mir-320 was merely 35% higher than that of mir-92.

3.4. Analysis of miRNA extracted from HeLa cells

The assay was applied to the analysis of the three miRNAs in total RNA extracted from HeLa cells to determine its ability in quantifying miRNAs in real world samples. The results were normalized to total RNA, as listed in Table 1. These results are in good agreement with Northern blot analysis on the same sample and consistent with recently published data of miRNA expression profiling (Barad et al., 2004; Allawi et al., 2004; Nelson et al., 2004). The lowest amount of total RNA needed for successful miRNA detections was found to be ~10 ng, corresponding to ~300 HeLa cells (Allawi et al., 2004; Lim et al., 2003). The relative errors associated with miRNA assays on individual miRNAs were generally less than 15% in the concentration range of 2.0–300 pM. Therefore, it allows us to identify miRNAs with less than two-fold difference in expression levels under two conditions. This is advantageous because the expressions of many of the most interesting miRNAs often differ lightly under different conditions. The proposed procedure offers a greater accuracy in the identification of differentially expressed miRNAs and cuts down on the need for running too many replicates. In addition, with the greatly improved sensitivity, the proposed method also significantly reduce the amount of total RNA needed from micrograms to nanograms.

4. Conclusions

The electrochemical miRNA assay described here is rapid, ultrasensitive, nonradioactive and is able to directly detect miRNA without involving biological ligation. By employing $Ru(PD)_2Cl_2$, miRNA was directly labeled with redox and electrocatalytic moieties under very mild conditions. Specific miRNA were detected amperometrically at subpicomolar levels

with high specificity. This electrochemical miRNA assay is easily extendable to a low-density array of 50–100 electrodes. The relatively limited number of miRNA offers excellent opportunity for low-density electrochemical arrays in miRNA assays. The advantages of low-density electrochemical biosensor arrays are: (i) more cost-effective than optical biosensor arrays; (ii) ultrasensitive when coupled with catalysis; (iii) rapid, direct, turbid and light absorbing-tolerant detection; (iv) portable, robust, low-cost, and easy-to-handle electrical components suitable for field tests and homecare use. Such a tool would be of great scientific value and may open the door to routine miRNA expression profiling and molecular diagnostics.

References

Allawi, H.T., Dahlberg, J.E., Olson, S., Lund, E., Olson, M., Ma, W.P., Takova, T., Neri, B.P., Lyamichev, V.I., 2004. RNA 10, 1153–1161.

Babak, T., Zhang, W., Morris, Q., Blencowe, B.J., Hughes, T.R., 2004. RNA 10, 1813–1819.

Barad, O., Meiri, E., Avniel, A., Aharonov, R., Barsilai, A., Bentwich, I., Einav, U., Gilad, S., Hurhan, P., Karov, Y., Lobenhofer, E.K., Sharon, E., Shiboleth, Y.M., Shtutman, M., Bentwich, Z., Einay, P., 2004. Genome Res. 14, 2486–2494.

Bard, A.J., Faulkner, L.R., 2001. Electrochemical Methods. John Willey & Sons, New York.

Bartel, D.P., 2004. Cell 116, 281–297.

Calin, G.A., Dumitru, C.D., Shimizu, M., Bichi, R., Zupo, S., Noch, E., Aldler, H., Rattan, S., Keating, M., Rai, K., 2002. Proc. Natl. Acad. Sci. U.S.A. 99, 15524–15529.

Calin, G.A., Liu, C.G., Sevignani, C., Ferracin, M., Felli, N., Dumitru, C.D., Shimizu, M., Cimmino, A., Zupo, S., Dono, M., 2004. Proc. Natl. Acad. Sci. U.S.A. 101, 11755–11760.

Caruso, F., Rodda, E., Furlong, D.N., Niikura, K., Okahata, Y., 1997. Anal. Chem. 69, 2043–2049.

Clarke, M.J., 2002. Coord. Chem. Rev. 232, 69–93.

Gao, Z., Tansil, N.C., 2005. Nucleic Acids Res. 33, e123.

Goss, C.A., Abruna, H.D., 1985. Inorg. Chem. 24, 4263–4267.

Gray, H.B., Winkler, J.R., 1996. Annu. Rev. Biochem. 65, 537–561.

Griffiths-Jones, S., 2004. Nucleic Acids Res. 32, D109–D111.

Hotze, A.C.G., Velders, A.H., Ugozzoli, F., Biagini-Cingi, M., Manotti-Lanfredi, A.M., Haasnoot, J.G., Reedijk, J., 2000. Inorg. Chem. 39, 3838–3844.

Lagos-Quintana, M., Rauhut, R., Lendeckel, W., Tuschl, T., 2001. Science 294, 853–858.

Lee, R.C., Ambros, V., 2001. Science 294, 862–864.

Liang, R.Q., Li, W., Li, Y., Tan, C.Y., Li, J.X., You-Xin Jin, Y.X., Ruan, K.C., 2005. Nucleic Acids Res. 33, e17.

Lim, L.P., Lau, N.C., Weinstein, E.G., Abdelhakim, A., Yekta, S., Roades, M.W., Burge, C.B., Bartel, D.P., 2003. Genes Dev. 17, 991–1008.

Liu, C.G., Calin, G.A., Meloon, B., Gamliel, N., Sevignani, C., Ferracin, M., Dumitru, C.D., Shimizu, M., Zupo, S., Dono, M., 2004. Proc. Natl. Acad. Sci. U.S.A. 101, 9740–9744.

Lu, J., Getz, G., Miska, E.A., Alvarez-Saavedra, E., Lamb, J., Peck, D., Sweet-Cordero, A., Ebert, B.L., Mak, R.H., Ferrando, A.A., Downing, J.R., Jacks, T., Horvitz, H.R., Golub, T.R., 2005. Nature 435, 834–838.

Nelson, P.T., Baldwin, D.A., Scearce, L.M., Oberholtzer, J.C., Tobias, J.W., Mourelatos, Z., 2004. Nat. Methods 1, 155–161.

Piunno, P.A.E., Krull, U.J., 2005. Anal. Bioanal. Chem. 381, 1004–1011.

Reinhart, B.J., Slack, F.J., Basson, M., Bettinger, J.C., Pasquinelli, T., Rougvie, A.E., Horvitz, H.R., Ruvkun, G., 2000. Nature 403, 901–906.

Schmittgen, T.D., Jiang, J., Liu, Q., Yang, L., 2004. Nucleic Acids Res. 32, e43.

Seddon, E.A., Seddon, K.R., 1984. The Chemistry of Ruthenium. Elsevier, Amsterdam.

Shi, M., Anson, F.C., 1998. Anal. Chem. 70, 1489–1495.

Tansil, N.C., Xie, H., Xie, F., Gao, Z., 2005. Anal. Chem. 77, 126–134.

Thomson, J.M., Parker, J., Perou, C.M., Hammond, S.M., 2004. Nat. Methods 1, 47–53.

Xie, H., Zhang, C., Gao, Z., 2004a. Anal. Chem. 76, 1611–1617.

Xie, H., Yu, Y.H., Xie, F., Lao, Y.Z., Gao, Z., 2004b. Anal. Chem. 76, 4023–4029.

Zhang, Y., Kim, H.H., Heller, A., 2003. Anal. Chem. 75, 3267–3269.